



ORIGINAL PAPER

MECHANISM OF ROCK BURST BASED ON ENERGY DISSIPATION THEORY AND ITS APPLICATIONS IN EROSION ZONE

Zhongcheng QIN, Tan LI^{*}, Qinghai LI, Guangbo CHEN and Bin CAO*College of Mining and Safety Engineering, Shandong University of Science and Technology, Qingdao, Shandong, 266590, China***Corresponding author's e-mail: litan597@163.com*

ARTICLE INFO

Article history:

Received 8 October 2018

Accepted 29 January 2019

Available online 28 February 2019

Keywords:

Rock burst

Erosion zone

Energy theory

Energy judgment coefficient

ABSTRACT

Rock burst is a common mine disaster often accompanied with casualties and property damage. An effective and accurate method for predicting rock burst is necessary. This paper proposed a method for predicting rock burst on the basis of energy theory. Firstly, according to the laws of energy distribution in the front of coalface, the energy judgment coefficient Q is proposed, the energy is not released to the outside when $Q < 0$, it means that the rock burst will not occur, the energy is released to the outside when $Q > 0$, it means that the rock burst may occur, the greater Q value is, the more energy is released to the outside when rock burst occurs. Secondly, based on the geological structure of erosion zone, the influence of the uniaxial compressive strength and pre-peak energy with the different of the height ratio, lithology, and dip angle are analyzed, it concluded that uniaxial compressive strength and pre-peak energy at the bottom of the erosion zone slope are greater and the uniaxial compressive strength and pre-peak energy at the edge of the erosion zone slope are smaller. Finally, taking the Xiaoyun Coal Mine as the engineering background, the energy judgment coefficient Q for predicting rock burst is applied. The results of the field observation are consistent with the results of the energy judgment coefficient Q . It indicates that this method can better predict the location and intensity of rock burst and provide a novel idea for preventing the occurrence of rock burst.

1. INTRODUCE

Rock burst is a complex mine disaster that is affected by many factors, which seriously threatens the safety of underground person and equipment during construction (Casten and Fajklewicz, 2010; Chen et al., 2012; Dou et al., 2014; Yan et al., 2015; Zhao et al., 2017). So far, more and more scholars have analyzed the instability mechanism of roadway surrounding rock based on energy, and considered that the occurrence of rock burst is caused by uneven energy distribution (Feng et al., 2012; Hajiabdomajid et al., 2002; Xie et al., 2004). Zhang et al. (2018) explored the mechanism of energy propagation and attenuation in rock medium and proposed a method to predict rock burst hazards using microseismic energy attenuation. Chen et al. (2013) selected the energy as an evaluation index for the rock burst intensity classification and proposed the rock burst intensity quantitative classification method. Guo et al. (2016) concluded that the combined structure of the upper hard thick conglomerate and the lower soft red layer could provide favorable conditions for the energy release. Yin et al. (2018) researched the evolution of energy stored in the composite coal-rock structure and coal fragments' burst characteristics through the lateral pressure unloading numerical tests, and they concluded that the accumulated strain energy in the coal was greater than that in roof and floor.

Rock burst is a sudden and violent release of the

elastic deformation energy accumulated in the rock mass under certain conditions, which causes the rock to burst and eject (Li et al., 2012; Pan et al., 2014). When the accumulated energy in the rock reaches the threshold, it can cause the crack initiation and crack damage (Ning et al., 2017). And the time curve of the total strain energy, elastic strain energy and dissipative strain energy have the remarkable periodical characteristics through the triaxial compression tests on hard rocks under different loading and unloading paths (Li et al., 2017). The process of energy accumulation and dissipation follows different laws (Weng et al., 2017).

However, there is little research on the energy distribution of coal seam erosion zone. The coal seam erosion zone generally refers to the erosion of the rock or coal layer by the river and seawater and is usually filled by sandy sediments (Hu et al., 2012). The erosion zone is a common geological phenomenon in the coal mine. The variation of coal seam thickness, angle and lithology of roof and floor caused by the erosion zone have a certain impact on the stress distribution (Pearson et al., 1990; Zhang et al., 2014).

Therefore, the variation of stress and energy in front of coalface are studied during mining in the erosion zone, and a new energy judgment method is proposed from the viewpoint of energy, which provides a novel thought for rock burst control in erosion zone.

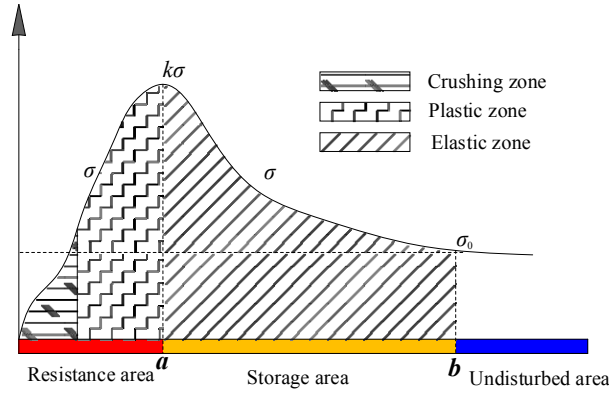


Fig. 1 Division of energy area in front of coalface.

2. ENERGY ANALYSIS

2.1. ENERGY JUDGMENT COEFFICIENT

During the formation process of the coal seam erosion zone, the original stress have formed a certain balanced distribution rule. The excavation of underground engineering will break the balanced state of original stress, and cause the redistribution of the stress and energy within a certain range. A lot of theoretical and practical research shows, the coal body in front of the coalface is divided into the crushing zone, plastic zone and elastic zone (Griffith et al., 2014; Zhao et al., 2010).

The coal with lots of macroscopic cracks in the crushing zone basically loses the bearing capacity and cannot accumulate lots of elastic deformation energy. The coal with a large plastic deformation, cracks and fissures in the plastic zone can have some bearing capacity and can accumulate some elastic deformation energy. The coal with few cracks in the elastic zone can accumulate lots of elastic deformation energy and provide the main energy during the rock burst.

Therefore, in the process of energy transfer and release, the elastic zone is the main source of energy release, the crushing zone and the plastic zone play the role of preventing the energy. Based on the above analysis, the area in front of the coalface is divided into energy release resistance zone, energy storage zone and unaffected zone, as shown in Figure 1.

According to the generalized Hooke Law, the elastic strain energy released from the unit rock mass under the triaxial compression test is (Xie et al., 2011):

$$U^e = \frac{1}{2E_0} [\sigma_1^2 + \sigma_2^2 + \sigma_3^2 - 2\nu(\sigma_1\sigma_2 + \sigma_2\sigma_3 + \sigma_1\sigma_3)] \quad (1)$$

Where U^e is the elastic strain energy released from unit rock mass, $\sigma_1, \sigma_2, \sigma_3$ are the three principal stresses of the rock unit, ν is the poisson's ratio and E_0 is elastic modulus, respectively.

The elastic strain energy of each unit in the storage area can be accumulated to obtain the total elastic strain energy of the rock mass. This paper proposes a new energy judgment coefficient (Q),

which refers to the ratio of the difference between the energy in the storage area U_s and the energy in the resistance area U_r to the energy in the storage area U_s in unit time. The size of the energy judgment coefficient directly reflects the proportion of energy released outward to the energy in the storage area. The formula can be expressed as:

$$Q = \frac{\frac{U_s - U_r}{t}}{\frac{U_s}{t}} = \frac{U_s - U_r}{U_s} \quad (2)$$

Where U_s is the energy in the storage area, which refers to how much energy is released outward. U_r is the energy in the resistance area, which refers to the ability to prevent energy releasing outward.

In addition, the energy judgment coefficient Q can be used to judge whether the rock burst occurred and the intensity of the rock burst, it can be expressed as:

$$\begin{cases} Q \geq 0 & \text{Energy release} \\ Q < 0 & \text{Energy does not release} \end{cases} \quad (3)$$

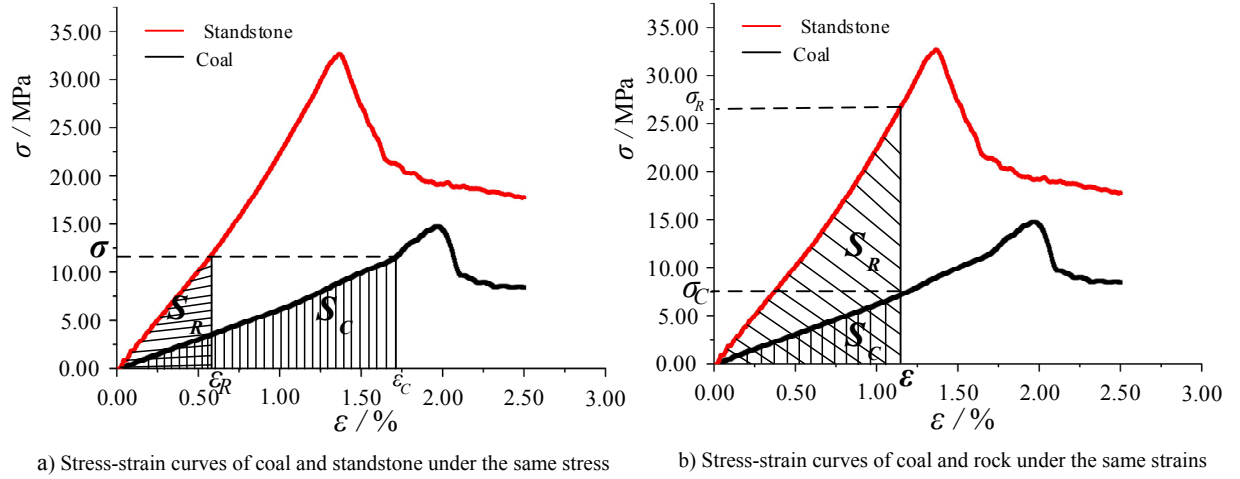
When $Q > 0$, the rock layer has the ability to release energy outward, and the energy released outward may cause rock burst, and the method of blasting and drilling can destroy the integrity of rock and reduce its ability to store elastic deformation energy, which can effectively prevent the occurrence of rock burst.

The greater the energy judgment coefficient is, the more the energy released when the rock burst occurs. The closer the Q value is to 1, the more energy released and the more serious the impact when the rock burst occurs.

In order to facilitate the judgment of rock burst on site, it is significance to establish a set of simple and direct mathematical functions to describe whether the rock burst occurred. Based on the above theoretical analysis, the functional relationship between the energy in the storage area and the distance from the coalface to the energy storage area is set as $f(x_s)$, and the functional relationship between the energy in the resistance area and the distance from

Table 1 Rock mechanics parameters.

Lithology	Density (kg/m)	Elastic Modulus (GPa)	Poisson Ratio	Friction Angle/ (°)	Cohesion (MPa)	Tensile Strength (MPa)
Medium Sand	2450	59.50	0.20	36	5.82	5.13
Fine Silt	2660	27.10	0.18	38	7.41	7.52
Coal	1680	3.52	0.19	28	3.77	2.05
Silt	2480	21.61	0.22	36	5.75	5.01
Fine Silt	2720	31.33	0.15	40	11.83	9.89
Mudstone	2130	16.73	0.24	37	3.95	1.91

**Fig. 2** Stress and strain curves of rock and coal specimens.

the coalface to the energy resistance area is set as $f(x_r)$, then the energy judgment coefficient Q can be expressed as:

$$Q = \frac{U_s - U_r}{U_s} = \frac{\int_a^b f(x_s) dx - \int_0^a f(x_r) dx}{\int_a^b f(x_s) dx} \quad (4)$$

2.2. COAL-ROCK COMBINED BODY TEST

2.2.1. UNIAXIAL COMPRESSION TEST

In order to study the energy storage state of rock and coal in the compression process, uniaxial compression tests are performed on the rock sample and the coal sample. The stress and strain curves in the compression process are shown in Figure 2, and the mechanical parameters of rock and coal are listed in Table 1. The S_C refers to the elastic deformation energy stored in the coal sample, the S_R refers to the elastic deformation energy stored in the rock sample. As shown in Figure 2a), the deformation of the coal sample is greater than that of the rock sample ($\epsilon_C > \epsilon_R$) and the elastic deformation energy stored in the coal sample is greater than that of the rock sample ($S_C > S_R$) when the same pressure σ is applied during the compression process. As shown in Figure 2b), when the pressure applied to the rock sample is greater than that of the coal sample ($\sigma_R > \sigma_C$), the energy stored in the rock sample is greater than that of the coal sample ($S_R > S_C$) and the coal sample and the rock sample generate the same deformation ($\epsilon_C = \epsilon_R$). So, in the same volume of coal sample and rock

sample, the coal sample can store more elastic deformation energy under the same pressure, the rock sample can store more elastic deformation energy when the same deformation is generated.

2.2.2. ORTHOGONAL TEST OF COAL-ROCK COMBINED BODY

In order to further analyze the compressive strength and pre-peak energy of coal-rock combined body, this paper chooses the height ratio, lithology, and slope angle as factors, select three levels for each factor, and conduct orthogonal test. By using the numerical simulation, the compressive strength and pre-peak accumulated energy of coal-rock combined body with different parameters were obtained. The uniaxial compressive strength and pre-peak energy are selected as the evaluation indicators. The mechanical parameters of rock and coal are listed in Table 1, the factors and the levels are listed in Table 2. The $L_9(3^4)$ orthogonal table is used in the test, the experimental program and the results of the orthogonal test are listed in Table 3.

2.2.3. RESULT ANALYSIS

(1) Range analysis

The method of range analysis can obtain the experimental conclusions through the comprehensive comparison of range analysis and drawing trend graphs (Yin et al., 2012). The range analysis of the uniaxial compressive strength and pre-peak energy are listed in Table 4 and Table 5 respectively.

Table 2 Factors and levels of orthogonal test.

Level	Height Ratio	Lithology	Slope Angle
1	1:2	Mudstone-Coal	0°
2	1:1	Fine Silt-Coal	30°
3	2:1	Medium Sand-Coal	45°

Table 3 Scheme for orthogonal test.

Number	Factors			Indicators	
	Height Ratio	Lithology	Slope Angle	Uniaxial Compressive Strength	Pre-peak Energy
1	1:2	Mudstone-Coal	0°	12.54	86.27
2	1:2	Fine Silt-Coal	30°	11.41	77.59
3	1:2	Medium Sand-Coal	45°	6.87	76.16
4	1:1	Mudstone-Coal	30°	11.60	90.41
5	1:1	Fine Silt-Coal	45°	6.16	32.03
6	1:1	Medium Sand-Coal	0°	12.23	68.43
7	2:1	Mudstone-Coal	45°	9.45	58.59
8	2:1	Fine Silt-Coal	0°	12.32	76.38
9	2:1	Medium Sand-Coal	30°	10.34	45.45

Table 4 Uniaxial compressive strength range analysis.

Factor	Height Ratio	Lithology	Slope Angle
Mean Value 1	10.273	11.197	12.363
Mean Value 2	9.997	9.963	11.117
Mean Value 3	10.703	9.813	7.493
Range	0.706	1.384	4.870

Table 5 Pre-peak energy range analysis.

Factor	Height Ratio	Lithology	Slope Angle
Mean Value 1	80.007	78.423	77.027
Mean Value 2	63.623	62.000	71.150
Mean Value 3	60.140	63.347	55.593
Range	19.867	16.423	21.434

As can be seen from Table 4, the order of range on the uniaxial compressive strength from big to small is: slope angle > lithology > height ratio. It indicates that the slope angle has the greatest impact on the uniaxial compressive strength of the coal-rock combined body, followed by the lithology and the coal-rock height ratio.

As can be seen from Table 5, the order of range on the pre-peak energy from big to small is: slope angle > height ratio > lithology. It indicates that the angle has the greatest impact on the pre-peak energy of coal-rock combined body, and the height ratio is the second highest and the lithology has the smallest impact.

(2) Variance analysis

The method of variance analysis can compare the fluctuation caused by the variation of the factor level with the fluctuation caused by the test error, and can be used as a supplement to the range analysis (Qin et al., 2016). The variance analysis of the uniaxial compressive strength and the pre-peak energy are listed in Table 6 and Table 7 respectively.

It can be found from the experiment results that

the three factors have a certain influence on the uniaxial compressive strength and pre-peak energy of the coal-rock combined body, but their significance is different. As shown from Table 6 and Table 7, the order of significance of the uniaxial compressive strength of each factor is: slope angle > lithology > height ratio; the order of significance of the pre-peak energy of each factor is: slope angle > height ratio > lithology.

In the ranking of various factors on the uniaxial compressive strength and pre-peak energy, the lithology and height ratio are ranked differently. The reason may be that the influence of the joint, the cracks and the discontinuous weak surface are not considered in the test.

2.3. ENERGY DISTRIBUTION LAW OF COAL SEAM EROSION ZONE

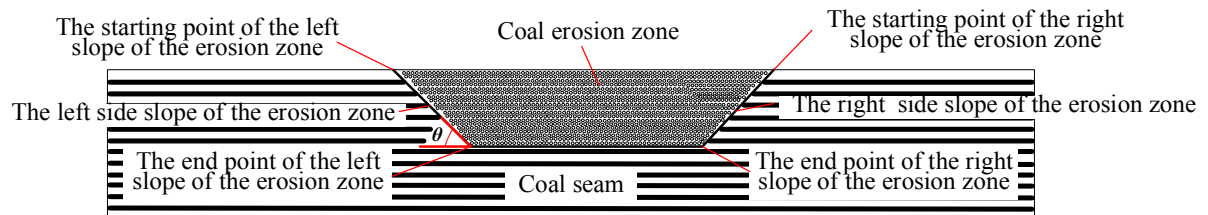
The erosion zone is a common geological phenomenon in the coal mine. The variation of coal seam thickness, angle and lithology of roof and floor caused by the erosion zone have a certain impact on the stress distribution. The schematic diagram of coal seam erosion zone is shown in Figure 3.

Table 6 Variance analysis of uniaxial compressive strength.

Factor	Square of Deviance	Degree of Freedom	F Ratio
Height Ratio	0.761	2	0.008
Lithology	3.457	2	0.036
Angle	38.400	2	0.401

Table 7 Variance analysis of pre-peak energy.

Factor	Square of Deviance	Degree of Freedom	F Ratio
Height Ratio	675.232	2	1.061
Lithology	498.845	2	0.784
Angle	735.933	2	1.156

**Fig. 3** Diagram of coal seam erosion zone.

Based on the above analysis of the experimental results of the coal-rock combined body, the FLAC^{3D} numerical simulation software is used to study the energy distribution of coal seam erosion zone. The size of the numerical simulation model is 200 m (length) \times 20 m (width) \times 60 m (high), the simulation buried depth is 600m, the vertical stress is 17.2 MPa, and the displacement of bottom surface is limited in the z direction. The lateral pressure coefficient is 0.8, the horizontal stress is applied 13.8 MPa in the x and y directions of the model, and the model is simulated by using the Mohr-Coulomb model. The mechanical parameters of each rock layer are listed in Table 1. Using the FLAC^{3D} numerical simulation software to study the followings:

(1) The thickness of the coal seam changes from 5m to 3m, the influence on the energy distribution when the slope angles are 3.43°, 4.29°, 5.72°, 8.53°, 16.70° is studied respectively. The elastic deformation energy distribution curve caused by the variation of the slope angle is shown in Figure 4;

(2) The slope angle is 14.04°, the influence on the energy distribution when the variation of coal thickness is 5-4-5, 5-3-5, 5-2-5, 5-1-5, 5-0-5 is studied respectively. The elastic deformation energy distribution curve caused by the variation of coal thickness is shown in Figure 5.

It can be seen from Figure 4 that the slope angle θ of erosion zone has a great influence on the distribution of the elastic deformation energy when the coal thickness is constant. The stress and the elastic deformation energy is low at the starting point of erosion zone slope, and the stress and the elastic deformation energy is higher at the end point of erosion zone slope. The greater the slope angle of erosion zone, the greater the amplitude of elastic

deformation energy on the erosion zone slope; the smaller the slope angle of erosion zone, the smaller the amplitude of the elastic deformation energy on the erosion zone slope.

It can be seen from Figure 5 that the variation of coal seam thickness has a great influence on the distribution of elastic deformation energy when the slope angle θ of the erosion zone is constant. The stress and the elastic deformation energy is low at the starting point of erosion zone slope, and the stress and the elastic deformation energy is higher at the end point of erosion zone slope. The greater the variation of coal thickness, the greater the amplitude of elastic deformation energy on the erosion zone slope; the smaller the variation of coal thickness, the smaller the amplitude of the elastic deformation energy on the erosion zone slope.

According to the above analysis, there is an inverse relationship between the rock stress and energy at the starting point of the erosion zone slope and the slope angle and coal thickness, and there is a direct relationship between the stress and stored energy at the end of the erosion zone slope and the slope angle and coal thickness.

3. THE ENGINEERING APPLICATION

3.1. GEOLOGICAL CONDITIONS

Xiaoyun coal mine is located in Jinxiang County, Jining City, Shandong Province, China, with the buried depth of 430 m-1500 m. The No.1314 coalface is located in the east wing in the mining area with a buried depth from 611 m to 665 m, and the coal seam thickness is 3.1-3.5 m, and coal seam dip is 10-18°. The immediate roof and floor are fine siltstone and siltstone respectively. Geological exploration shows that the coal seam in the area is brittle and hard, with

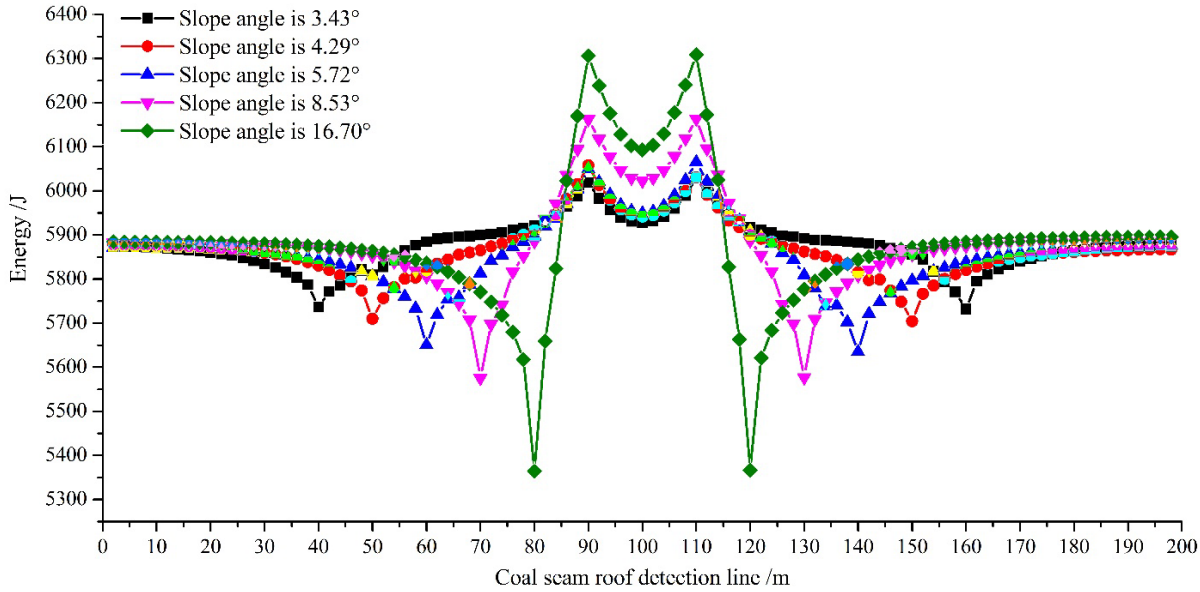


Fig. 4 Energy distribution curve of roof monitoring line in different slope angle.

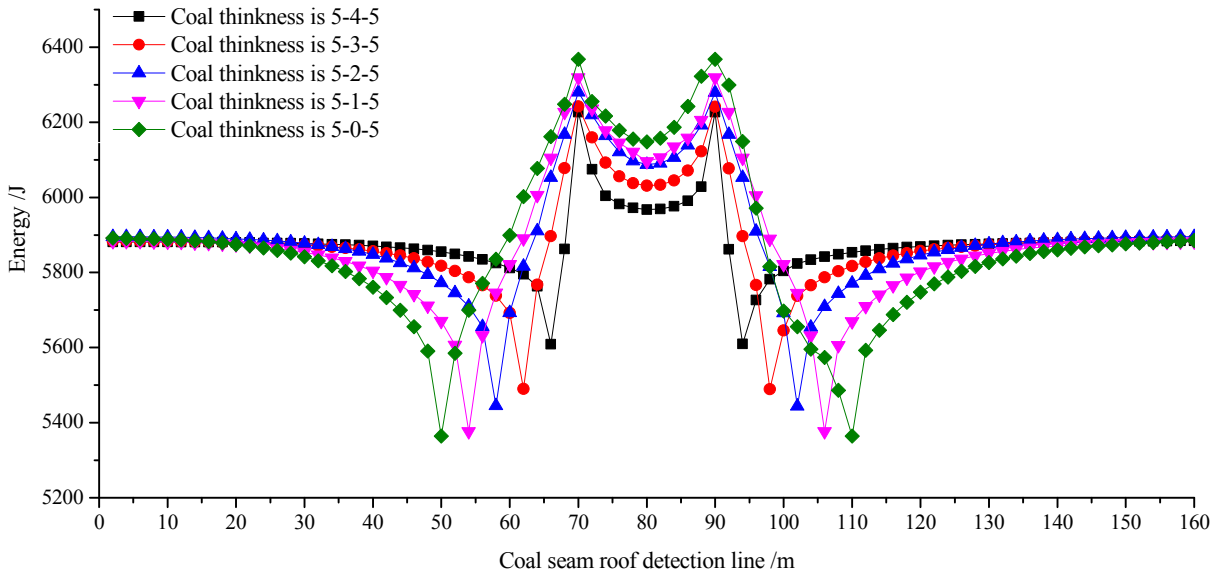


Fig. 5 Energy distribution curve of roof monitoring line in different coal thickness.

the ability to accumulate a large amount of elastic energy. There is a sandstone erosion zone in the middle of the mining area, as shown in Figure 6.

3.2. THE NUMERICAL MODEL

The variation of stress and energy caused by the mining in erosion zone is analyzed and studied by using the FLAC^{3D} numerical simulation software. The size of the model is 200m (length) \times 20m (thickness) \times 60m (height). The stress detection line is set at the junction of the immediate roof and the coal seam. The immediate roof is fine siltstone, main roof is medium sandstone, the bottom floor is siltstone. The coal seam thickness in the erosion zone is 0-3 m, and there is a 2 m coal seam thickness at the lower of erosion zone. The upper width, the lower part width, and the height of the erosion zone are 60 m, 20 m and 5 m respectively, as shown in Figure 7. The top surface of the model is set the free face and the displacement of bottom surface is limited. It simulates the pressure at

a depth of 650 m, the vertical stress is 17.2 MPa. The lateral pressure coefficient of the model is 0.8, the horizontal stress is applied 13.8 MPa in the x and y directions of the model, and the model is the Mohr-Coulomb model. The mechanical parameters of each rock layer are listed in Table 1.

3.3. THE ENERGY DISTRIBUTION IN MINING PROCESS

The process of 1314 coalface passing through erosion zone includes three processes: entering the erosion zone, in the erosion zone, leaving the erosion zone. The mining method of full-thickness excavation along the floor is employed in the 1314 coalface. The 11 representative coalface positions are selected in the process of coalface passing through erosion zone, the vertical stress distribution in front of the coalface is analyzed and studied. This paper studied the distribution characteristics of vertical stress and the advanced support pressure in the coal seam erosion

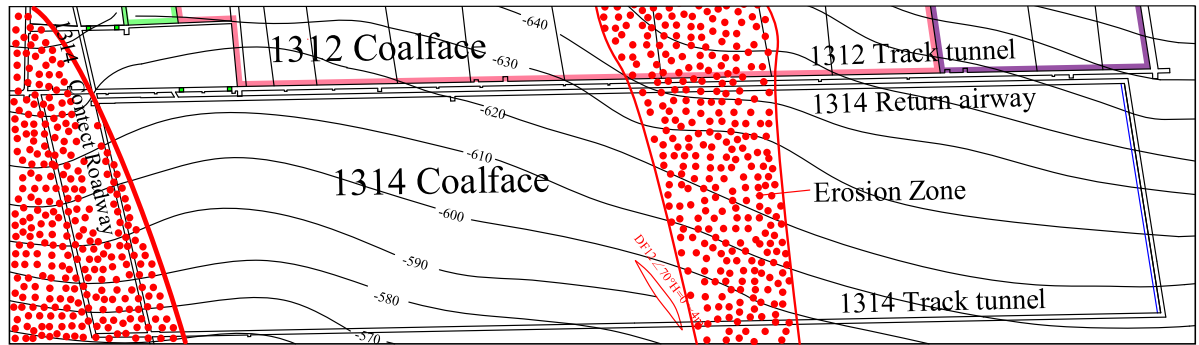


Fig. 6 The layout of No. 1314 coalface.

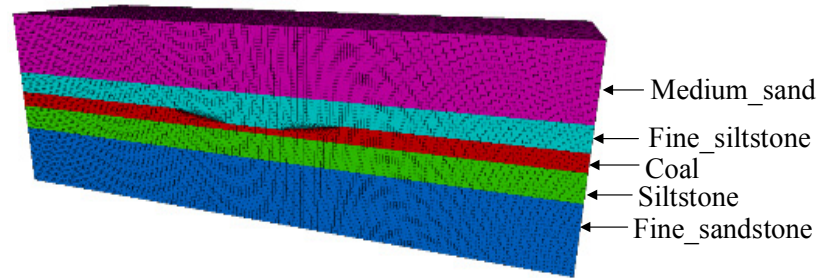


Fig. 7 The numerical model.

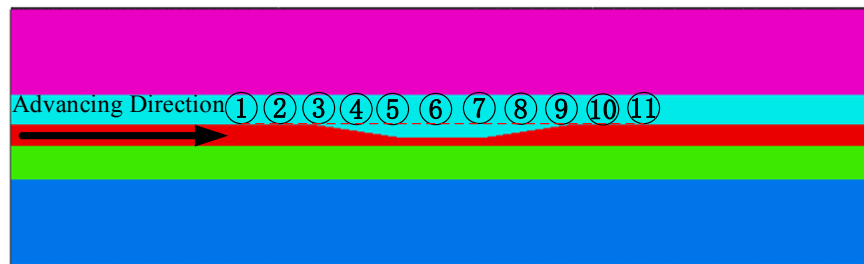


Fig. 8 Schematic of coalface position 1-11.

zone, and provided a basis for the energy distribution of the erosion zone. The coalface position 1-11 is shown in Figure 8.

The energy accumulation formed by erosion zone structure is called internal energy environments. The energy accumulation generated by mining is called the external energy environment. As the coalface moves forward, the advanced support pressure area will move forward. When the external energy environment produced by the advanced support pressure and the internal energy environment formed by the erosion zone structure meet and overlap with each other, it will form the high stress area in front of the coalface, and the stored energy will also accumulate and increase in this area, as shown in Figure 9. When the energy stored in the storage area is greater than the energy stored in the resistance zone, the energy of the storage area have the ability to overcome the energy of the resistance zone, and then the residual energy will be released to the excavation space, the rock burst maybe occur. The stress

distribution in front of the coalface from position 1 to position 11 during the mining process is shown in Figure 10 (a). As the figure shown, the range of resistance area in front of the coalface is about 10 m, and the range of energy storage area in front of the coalface is about 25 m. The peak value of the advanced support pressure is shown in Figure 10 (b). The maximum peak value is at positions 4 and 8 and the minimum peak value is at positions 3 and 9. It indicates that the stress peak value produced in the middle of the erosion zone slope is higher, and the stress peak value at the edge of the erosion zone slope is lower. The stress peak value at position 4 is slightly higher than that at position 8; it indicates that the stress peak value of the coalface entering the erosion zone is higher than that of the coalface leaving the erosion zone.

During the No.1314 coalface mining process, the function of the energy in front of the coalface and the coalface advanced distance is fitted, as shown in Figure 11. Where the $f(x_s)$ represents the energy

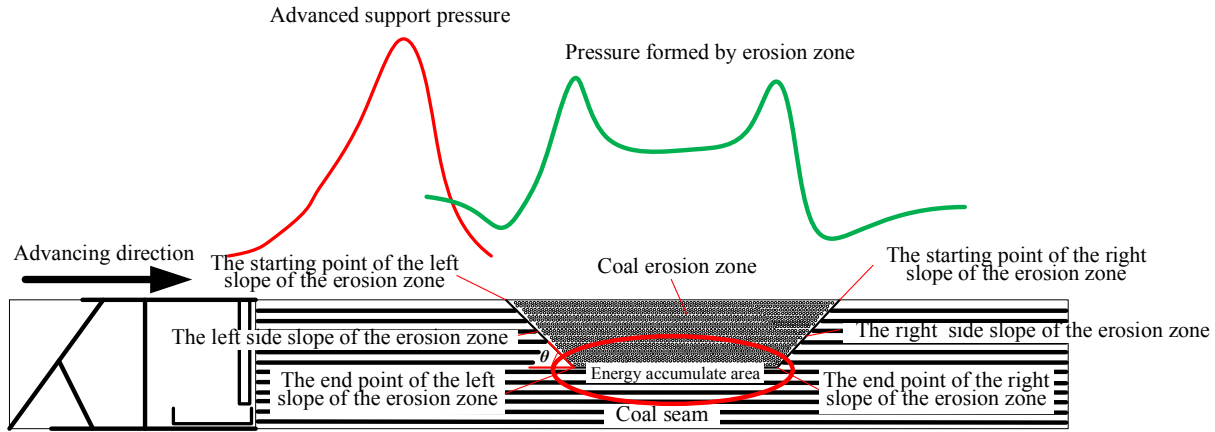


Fig. 9 Schematic diagram of the energy distribution of the coalface into the flush zone.

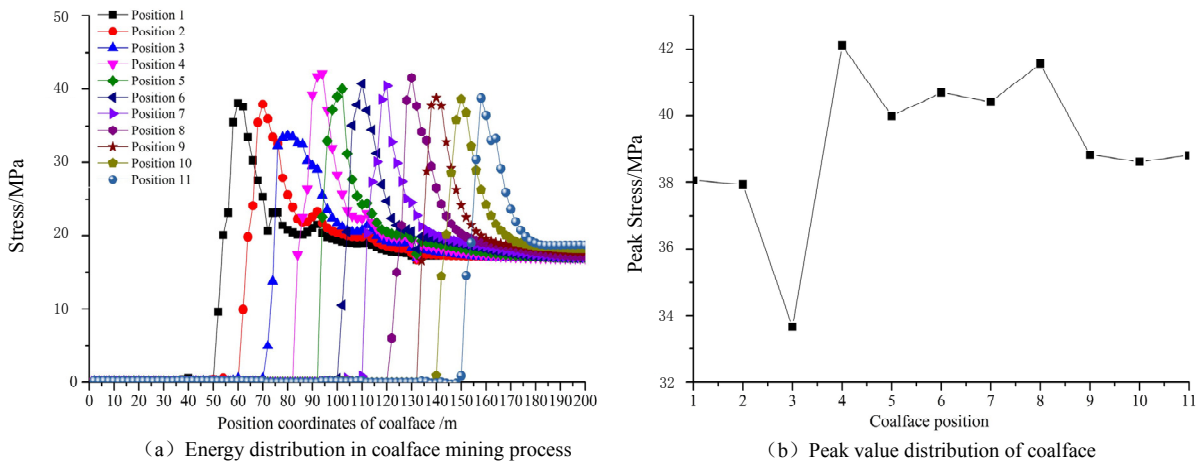


Fig. 10 Stress distribution in the mining process.

function of the storage area, the $f(x_r)$ represents the energy function of the resistance area.

According to the equation (4) and the energy fitting function during the mining process, the energy in the storage zone (U_s), the energy in the resistance zone (U_r) and the energy determination coefficient (Q) at the positions 1-11 are calculated, respectively. The calculated results are listed in Table 8.

As the coalface moves from position 1 to position 11, the elastic deformation energy of the storage zone and resistance zone in front of the coalface have changed significantly, as can be seen from Figure 12. It can be seen that there are three peaks of position 4, position 6 and position 8 during the mining in the erosion zone, the positions 4 and 8 are in the middle of the erosion zone slope and position 6 is in the middle of the erosion zone. But the reasons for the three peaks are different. The energy storage area is in the bottom area of the erosion zone when coalface is at position 4, the height ratio of coal and rock is small, the characteristics of the energy storage zone at position 4 is that the lithology is sandstone and coal, and the slope angle is 0° , which can store more elastic deformation energy. The energy storage area is at the slope of the erosion zone when coalface is at position 6, the characteristics of the energy storage zone at position 6 is that the height

ratio of coal and rock is bigger, the lithology is sandstone and coal, and the slope angle is 8.53° , which can store some elastic deformation energy. The energy storage area is not in the influence range of the erosion zone when coalface is at the position 8, the characteristics of the energy storage zone at position 8 is that lithology is the coal, which can produce certain deformation and store some elastic deformation energy. It can be seen from Table 8 that the energy in the storage area at the position 4, position 6 and position 8 is 355247.72 J, 298035.98 J and 288582.04 J respectively, and the energy at these three positions shows a decreasing trend. Meanwhile, the energy in the storage area is lower when the coalface is at position 2, position 5, position 7 and position 10. The energy storage area is at the range of erosion zone slope when coalface is at the position 2, the characteristics of the energy storage zone at the position 2 is that the height ratio of coal and rock is gradually becoming small, the lithology is sandstone and coal, and the slope angle is 8.53° , which can store less elastic deformation energy. The part of the energy storage area is at the bottom of the erosion zone and the other part is at the slope of the erosion zone when coalface is at the position 5, the characteristics of the energy storage zone at the position 5 is that the height ratio of coal and rock is gradually becoming big, the

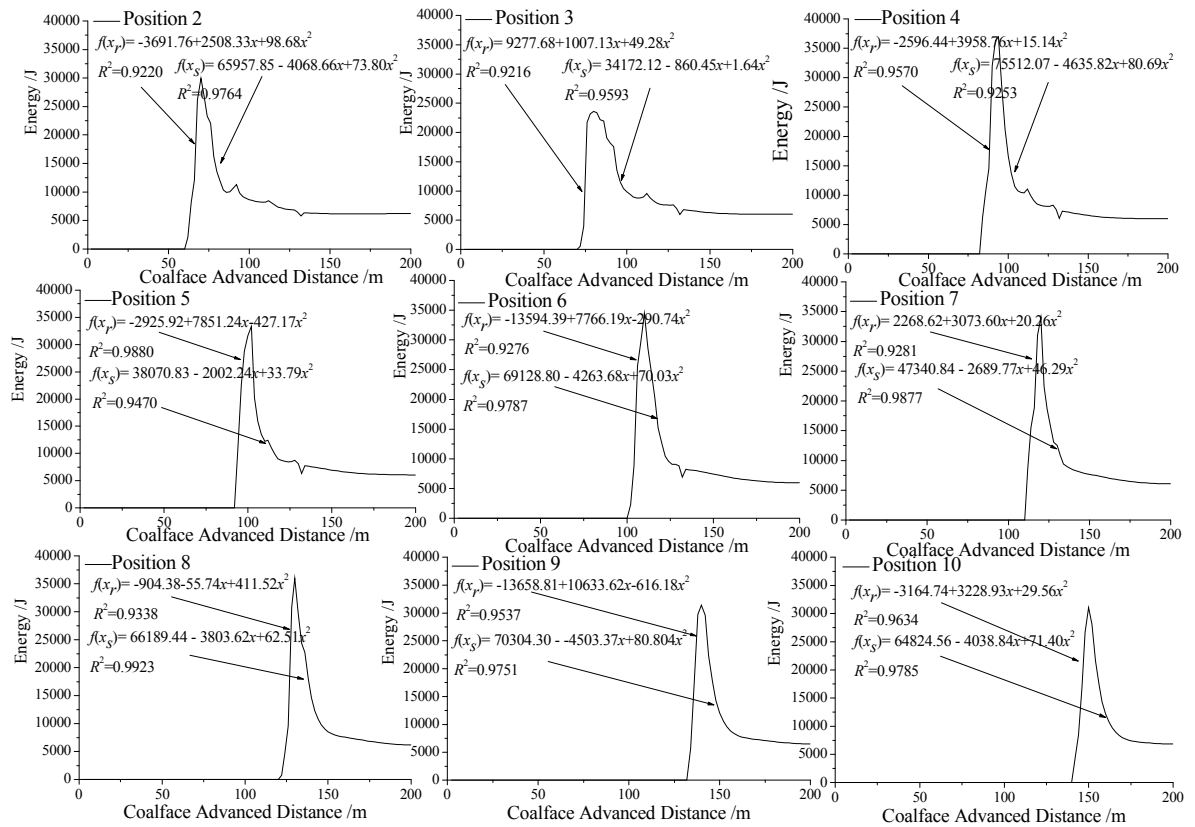


Fig. 11 The fitting function of position 2-10.

Table 8 Energy judgment coefficient during mining process.

Number	Coalface position information	U_s	U_r	Q
1	20 m from the starting point of the left slope of the erosion zone	183641.96	193186.43	-0.0520
2	10 m from the starting point of the left slope of the erosion zone	138621.71	193139.52	-0.3933
3	the starting point of the left slope of the erosion zone	269601.63	159559.70	0.4082
4	the middle of the left slope of the erosion zone	355247.72	105613.46	0.7027
5	the end point of the left slope of the erosion zone	205259.31	154927.40	0.2452
6	the middle of the bottom of the erosion zone	298035.98	90142.54	0.6975
7	the end point of the right slope of the erosion zone	231751.49	119962.90	0.4824
8	the middle of the right slope of the erosion zone	288582.04	125341.03	0.5657
9	the starting point of the right slope of the erosion zone	216075.16	189700.27	0.1221
10	10 m from the starting point of the right slope of the erosion zone	112904.24	139654.13	-0.2369
11	20 m from the starting point of the right slope of the erosion zone	170271.81	175183.75	-0.0288

lithology is becoming from sandstone and coal to coal, and the slope angle is increased from 0 to 8.53, which can store less elastic deformation energy. The part of energy storage area is at the slope of the erosion zone and the other part is at the full coal out of the erosion zone when coalface is at position 7, the characteristics of the energy storage zone at the position 7 is that the height ratio of coal and rock increases to the maximum, and the angle of dip is decreased from 8.53° to 0°, which can store less elastic deformation energy. It can be seen from the energy curve of the storage area and the resistance area in front of the coalface, the energy curve of the resistance area is lower than the energy curve of the storage area within the range of influence of the erosion zone. The energy in resistance zone mainly

refers to the energy stored in the crushing area and plastic area in front of the coalface. Through the analysis of the energy curve of the resistance zone, it can be found that the energy in the resistance zone at position 5 and 9 is higher. The energy resistance area is at the bottom of the erosion zone when coalface is at the position 5, the characteristics of this area are thicker sandstones, less fragmentation, and the ability to store large amounts of energy. The reason that the energy of the resistance zone is low at position 6 is that the range of resistance zone is at the high stress concentration zone of the bottom of the erosion zone, which the rock has a high fragmentation degree and cannot have the conditions of storing more energy.

According to the judgment of formula (3), there is the possibility of the rock burst when the energy

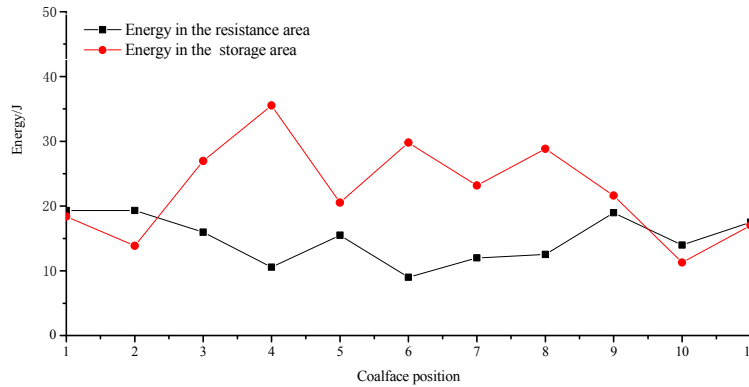


Fig. 12 Energy curve of storage area and resistance area.

judgment coefficient $Q > 0$. The higher the Q value, the greater the possibility of rock burst. When coalface is mined from position 2 to position 4, the energy judgment coefficient Q shows an increasing trend. When coalface is mined from position 4 to position 5, the energy judgment coefficient Q shows a decreasing trend. When coalface is at position 4, the energy judgment coefficient Q is maximum. The coalface is mined from position 5 to position 7, the energy judgment coefficient Q shows the trend of increasing first and then decreasing, the energy judgment coefficient Q is the largest when coalface is at the position 6. The coalface is mined from position 7 to position 9, the energy judgment coefficient Q shows a trend of increasing first and then decreasing, the coefficient of energy judgment Q is the largest when coalface is at the position 8. As the coalface is far away from the erosion zone, the energy judgment coefficient Q is decreased. And the energy judgment coefficient Q at the positions 4, position 6, and position 8 shows a decreasing trend, which means that the surrounding rock releases more energy when the coalface enters the erosion zone. The risk of rock burst is higher when the coalface enters the erosion zone.

4. FIELD MONITORING

Real-time monitoring of the No.1314 coalface is employed by the microseismic monitoring system. The source location, microseismic energy and are calculated every day. The relationship between the total microseismic energy, the microseismic frequency and the coalface advance time is shown in Figure 14. It can be seen that the value of total microseismic energy and microseismic frequency when the coalface enters the erosion zone are bigger than that of the coalface leaves the erosion zone. When the coalface enters the erosion zone slope, the field workers heard the huge rock broken sounds in the rock body, and the large cracks appeared on the roadway surrounding surface. It indicates that there is more energy released in this range, and there is a greater possibility of occurrence of rock burst, the results of the field

microseismic monitoring are consistent with the above analysis.

5. DISCUSSION

The occurrence of rock burst is accompanied by the release of energy. The purpose of this paper is to propose an effective method to predict rock burst based on the viewpoint of energy.

(1) This paper proposed an energy judgment coefficient Q to predict the rock burst. The greater the energy judgment coefficient Q is, the more energy is released outward, the greater the possibility of the occurrence of rock burst. In addition, energy judgment coefficient Q is helpful to choose reasonable supporting form of roadway based on the magnitude of the energy released outside. However, the numerical simulation software has certain limitations, the simulated rock is continuous and homogeneous, but the actual rock is discontinuous and heterogeneous. Therefore, there is a gap compared with the actual situation.

(2) Based on the structural properties of the erosion zone, the law of energy distribution near the erosion zone is analyzed. The energy at the edge of the erosion zone is low, the energy in the interior of the erosion zone is high. The possibility of rock burst in the interior of the erosion zone is greater than that at the edge of the erosion zone, and the energy judgment coefficient of the coalface entering the erosion zone is greater than that of leaving erosion zone. It has certain guiding significance to prevent rock burst in the process of coalface passing through the erosion zone.

(3) The results of the rock burst predicted by the energy judgment coefficient are consistent with the results of the microseismic monitoring, it indicates that this new method of predicting rock burst is reliable and accurate. However, there are some limitations because these conclusions are obtained by monitoring the No.1314 coalface of Xiaoyun Coal Mine, and the monitoring conclusions of other coal mines are not yet known. So it is also necessary to apply and analysis this method to other coal mines in the future.

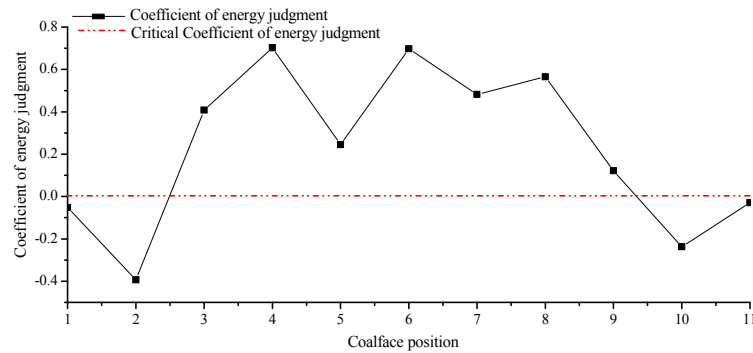


Fig. 13 Energy judgment coefficient curve.

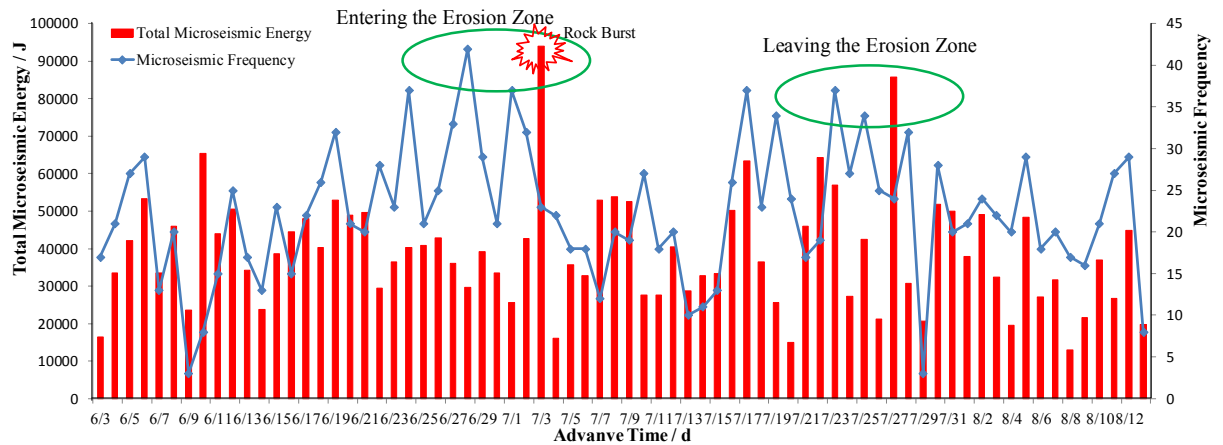


Fig. 14 Microseismic energy statistics in mining process.

6. CONCLUSIONS

(1) Based on the characteristics of energy distribution in front of the coalface, the energy judgment coefficient Q is established. When $Q > 0$, the rock burst may occur; when $Q < 0$, the rock burst may not occur. The magnitude of the Q value can reflect the severity of the rock burst, and the greater the Q is, the more violent the impact is.

(2) According to the results of the orthogonal test of the coal-rock combined body, the influence degree and significance of the uniaxial compressive strength of coal-rock combined body as follows: angle > lithology > height ratio, the influence degree and significance of the pre-peak energy of coal-rock combined body as follows: angle > height ratio > lithology.

(3) The slope angle of the erosion zone has a significant influence on the energy distribution. There is an inverse relationship between the energy at the starting point of the erosion zone slope and the slope angle and the coal thickness variation of the erosion zone. And the energy at the end of the erosion zone slope is proportional to the slope angle of the erosion zone and the coal thickness variation. The energy at the starting point of the erosion zone slope is the minimum and the energy at the end point of the erosion zone slope is the maximum. The energy accumulated in the erosion zone is higher than that

outside of the erosion zone. The greater the variation of the erosion zone slope, the greater the difference of energy between the starting point and the end point of the erosion zone slope.

(4) The energy judgment coefficient is greatest when the coalface is at the bottom of the erosion zone and the middle part of the erosion zone slope. The energy judgment coefficient of the coalface entering the erosion zone is greater than that of leaving erosion zone. The results of the rock burst predicted by the energy judgment coefficient are consistent with the results of the microseismic monitoring. This method provides a new idea for preventing the occurrence of the rock burst.

DATA AVAILABILITY STATEMENT

The authors declare that all data supporting the findings of this study are available within the article, the reader can find and use it, there is no unavailable data.

ACKNOWLEDGEMENTS

This study was supported by the National Natural Science Foundation of China [grant numbers 51604164]; and by the program of youth teacher growth plan in Shandong province.

REFERENCES

- Casten, U. and Fajkiewicz, Z.: 2010, Induced gravity anomalies and rock-burst risk in coal mines: a case history. *Geophysical Prospecting*, 41, No. 1, 1–13. DOI: 10.1111/j.1365-2478.1993.tb00562.x
- Chen, B.R., Feng, X.T., Li, Q.P., Luo, R.Z. and Li, S.J.: 2013, Rock burst intensity classification based on the radiated energy with damage intensity at Jinping II Hydropower Station, China. *Rock Mechanics and Rock Engineering*, 48, No. 1, 289–303. DOI: 10.1007/s00603-013-0524-2
- Chen, X.H., Li, W.Q. and Yan, X.Y.: 2012, Analysis on rock burst danger when fully-mechanized caving coal face passed fault with deep mining. *Safety Science*, 50, No. 4, 645–648. DOI: 10.1016/j.ssci.2011.08.063
- Dou, L.M., He, X.Q., He, H., He, J. and Fan, J.: 2014, Spatial structure evolution of overlying strata and inducing mechanism of rockburst in coal mine. *Transactions of Nonferrous Metals Society of China*, 24, No. 4, 1255–1261. DOI: 10.1016/S1003-6326(14)63187-3
- Feng, G.L., Feng, X.T., Chen, B.R., Xiao, Y.X. and Yu, Y.: 2015, A microseismic method for dynamic warning of rockburst development processes in tunnels. *Rock Mechanics and Rock Engineering*, 48, No. 5, 2061–2076. DOI: 10.1007/s00603-014-0689-3
- Griffith, W.A., Becker, J., Cione, K., Miller, T. and Pan, E.: 2014, 3D topographic stress perturbations and implications for ground control in underground coal mines. *International Journal of Rock Mechanics and Mining Sciences*, 70, 59–68. DOI: 10.1016/j.ijrmms.2014.03.013
- Guo, W.J., Li, Y.C., Yin, D.W., Zhang, S.C. and Sun, X.Z.: 2016, Mechanisms of rock burst in hard and thick upper strata and rock-burst controlling technology. *Arabian Journal of Geosciences*, 9, No. 10, 561. DOI: 10.1007/s12517-016-2596-2
- Hajiabdolmajid, V., Kaiser, P.K. and Martin, C.D.: 2002, Modeling brittle failure of rock. *International Journal of Rock Mechanics and Mining Sciences*, 39, No. 6, 731–741. DOI: 10.1016/S1365-1609(02)00051-5
- Hu, Y.B., Wu, Y.Q., Kang, H.Q. and Fu, G.H.: 2012, Application of the mine multi-wave seismograph in the measurement of coal seam washout zone. *Applied Mechanics and Materials*, 103, 20–24. DOI: 10.4028/www.scientific.net/AMM.103.20
- Li, S.J., Feng, X.T., Li, Z.H., Chen, B.R., Zhang, C.Q. and Zhou, H.: 2012, In situ monitoring of rockburst nucleation and evolution in the deeply buried tunnels of Jinping II hydropower station. *Engineering Geology*, 137, No. 7, 85–96. DOI: 10.1016/j.enggeo.2012.03.010
- Li, T.B., Ma, C.C., Zhu, M.L. Meng, L.B. and Chen, G.Q.: 2017, Geomechanical types and mechanical analyses of rockbursts. *Engineering Geology*, 222, 72–83. DOI: 10.1016/j.enggeo.2017.03.011
- Ning, J.G., Wang, J., Jiang, J.Q., Hu, S.C., Jiang, L.S. and Liu, X.S.: 2017, Estimation of crack initiation and propagation thresholds of confined brittle coal specimens based on energy dissipation theory. *Rock Mechanics and Rock Engineering*, 51, No. 5, 1–16. DOI: 10.1007/s00603-017-1317-9
- Pan, Y.S., Xiao, Y.H., Li, Z.H. and Wang, K.X.: 2014, Study of tunnel support theory of rockburst in coal mine and its application. *Journal of China Coal Society*, 39, No. 2, 222–228. DOI: 10.13225/j.cnki.jccs.2013.2015
- Pearson, J. and Murchison, D.G.: 1990, Influence of a sandstone washout on the properties of an underlying coal seam. *Fuel*, 69, No. 2, 251–253. DOI: 10.1016/0016-2361(90)90182-P
- Qin, Z.C., Yu, X., Li, Q.H., Zhang, P.S., Huang, D.M. and Zhi, J.: 2016, Study on the orthogonal numerical simulation experiment of the effect of surrounding rock mechanical parameters on roadway deformation and failure. *Journal of Mining and Safety Engineering*, 33, No. 1, 77–82. DOI: 10.13545/j.cnki.jmse.2016.01.012
- Weng, L., Huang, L.Q., Taheri, A. and Li, X.: 2017, Rockburst characteristics and numerical simulation based on a strain energy density index: A case study of a roadway in Linglong gold mine, China. *Tunnelling and Underground Space Technology*, 69, 223–232. DOI: 10.1016/j.tust.2017.05.011
- Xie, H., Peng, R.D. and Yang, J.: 2004, Energy dissipation of rock deformation and fracture. *Chinese Journal of Rock Mechanics and Engineering*, 23, No. 21, 3565–3570.
- Xie, H.P., Li, L., Ju, Y.Y., Peng, R.D. and Yang, Y.M.: 2011, Energy analysis for damage and catastrophic failure of rocks. *Science China Technological Sciences*, 54, No. 1, 199–209. DOI: 10.1007/s11431-011-4639-y
- Yan, P., Zhao, Z.G., Lu, W.B., Fan, Y., Chen, X.R. and Shan, Z.G.: 2015, Mitigation of rock burst events by blasting techniques during deep-tunnel excavation. *Engineering Geology*, 188, 126–136. DOI: 10.1016/j.enggeo.2015.01.011
- Yin, S.H., Wu, A.X. and Li, X.W.: 2012, Orthogonal polar difference analysis for sensitivity of the factors influencing the ore pillar stability. *Journal of China Coal Society*, 37, No. 1, 48–52. DOI: 10.13225/j.cnki.jccs.2012.s1.021
- Yin, Y.C., Tan, Y.L., Lu, Y.W. and Zhang, Y.B.: 2018, Numerical research on energy evolution and burst behavior of unloading coal-rock composite structures. *Geotechnical and Geological Engineering*, 37, 295–303. DOI: 10.1007/s10706-018-0609-5
- Zhang, F., Wang, P., Chen, Z.J. and Xi, A.L.: 2014, Mixture distribution of coal seam thickness and its significance in Zhongji exploration zone of Yulin-Shenmu mining district in northern Shaanxi. *Journal of Geology*, 38, No. 03, 399–407. DOI: 10.3969/j.issn.1674-3636.2014.03.399
- Zhang, M.W., Liu, S.D. and Shimada, H.: 2018, Regional hazard prediction of rock bursts using microseismic energy attenuation tomography in deep mining. *Natural Hazards*, 93, No. 3, 1359–1378. DOI: 10.1007/s11069-018-3355-3
- Zhao, G.B., Wang, D., Gao, Y.B. and Wang, S.J.: 2017, Modifying rock burst criteria based on observations in a division tunnel. *Engineering Geology*, 216, 153–160. DOI: 10.1016/j.enggeo.2016.11.014
- Zhao, Y.X., Jiang, Y.D. and Tian, S.P.: 2010, Investigation on the characteristics of energy dissipation in the preparation process of coal bumps. *Journal of China Coal Society*, 35, No. 12, 1979–1983. DOI: 10.1016/S1876-3804(11)60004-9